

# Simulation of Back-Electrode Effects on Lags and Current Collapse in Field-Plate AlGaN/GaN HEMTs

K. Horio, H. Onodera and T. Fukai

Faculty of Systems Engineering, Shibaura Institute of Technology  
307 Fukasaku, Saitama 337-8570, Japan, horio@sic.shibaura-it.ac.jp

## ABSTRACT

Two-dimensional transient analysis of field-plate AlGaN/GaN HEMTs with a back electrode is performed by considering a deep donor and a deep acceptor in a buffer layer. It is shown that the introduction of field plate is effective in reducing current collapse when the acceptor density is high. On the other hand, the introduction of back electrode is effective in reducing current collapse particularly when the acceptor density is relatively low. It is also shown that applying a negative voltage to the back electrode is not so effective in reducing current collapse when the deep donor acts as an electron trap.

**Keywords:** GaN, HEMT, current collapse, field plate, back electrode

## 1 INTRODUCTION

In AlGaN/GaN HEMTs, slow current transients are often observed even if the drain voltage  $V_D$  or the gate voltage  $V_G$  is changed abruptly [1]. This is called drain lag or gate lag. Slow current transients indicate that dc  $I$ - $V$  curves and RF  $I$ - $V$  curves become quite different, resulting in lower RF power available than that expected from dc operation. This is called current collapse [2]. The use of field-plate structure, where the gate electrode extends onto surface passivation layer (cf. Fig.1), is considered to reduce surface-related current collapse [3], but its effects on buffer-related current collapse are not well known [4]. On the other hand, a recent experimental study shows that putting a back electrode under a buffer layer reduces the current collapse [5]. This indicates the importance of buffer-related current collapse [6]. Therefore, in this work, we perform two-dimensional analysis of field-plate AlGaN/GaN HEMTs with a back electrode and study how and when the buffer-related current collapse is reduced.

## 2 PHYSICAL MODELS

Fig.1 shows a device structure analyzed in this study. The gate length is  $0.3 \mu\text{m}$ . Note that the gate electrode extends onto SiN passivation layer. This is called a gate field plate. The field-plate length  $L_{FP}$  is typically set to  $1 \mu\text{m}$ . The thickness of SiN passivation layer  $d$  is typically set to  $30 \text{ nm}$ . The potential of back electrode  $V_B$  is normally fixed to  $0 \text{ V}$ , but it varied between  $0$  and  $-20 \text{ V}$ .

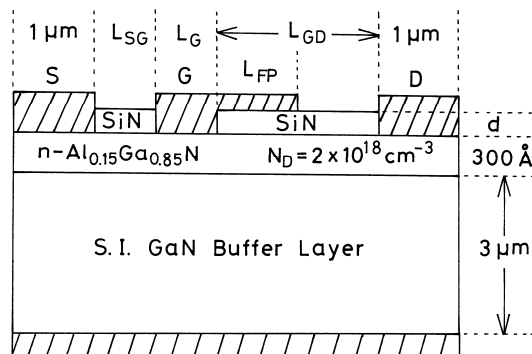


Figure 1: Device structure analyzed in this study.

In a buffer layer, we consider a deep donor and a deep acceptor [7, 8]. The deep acceptor's energy level is set  $0.6 \text{ eV}$  above the top of valence band. The deep donor's energy level is typically set to  $1 \text{ eV}$  below the bottom of conduction band [8]. The deep-acceptor density  $N_{DA}$  is varied between  $5 \times 10^{15} \text{ cm}^{-3}$  and  $10^{17} \text{ cm}^{-3}$ . The deep-donor density  $N_{DD}$  is set higher than the deep-acceptor density  $N_{DA}$ . In this case, the deep donors donate electrons to the deep acceptors, and hence the ionized deep-donor density  $N_{DD}^+$  becomes nearly equal to  $N_{DA}$  under equilibrium, and the deep donors act as electron traps. The steepness of energy barrier at the channel-buffer interface is determined by  $N_{DA}$ , and the energy barrier becomes steeper when  $N_{DA}$  is higher.

Basic equations are Poisson's equation including ionized deep-level terms, continuity equations for electrons and holes including carrier loss rates via the deep levels, and rate equations for the deep levels [8]. These equations are put into discrete forms and solved numerically. We calculate drain-current responses of AlGaN/GaN/HEMTs when the drain voltage  $V_D$  and/or the gate voltage  $V_G$  are changed abruptly.

## 3 CASE WITH HIGH ACCEPTOR DENSITY IN THE BUFFER LAYER

Fig.2 shows a comparison of calculated drain-current responses of two AlGaN/GaN HEMTs when  $V_D$  is lowered abruptly from  $40 \text{ V}$  to  $V_{Dfm}$  and  $V_G$  is kept constant at  $0 \text{ V}$ . Here,  $N_{DA} = 10^{17} \text{ cm}^{-3}$ . Fig.2(a) shows the case of normal structure without a field plate and a back electrode, and

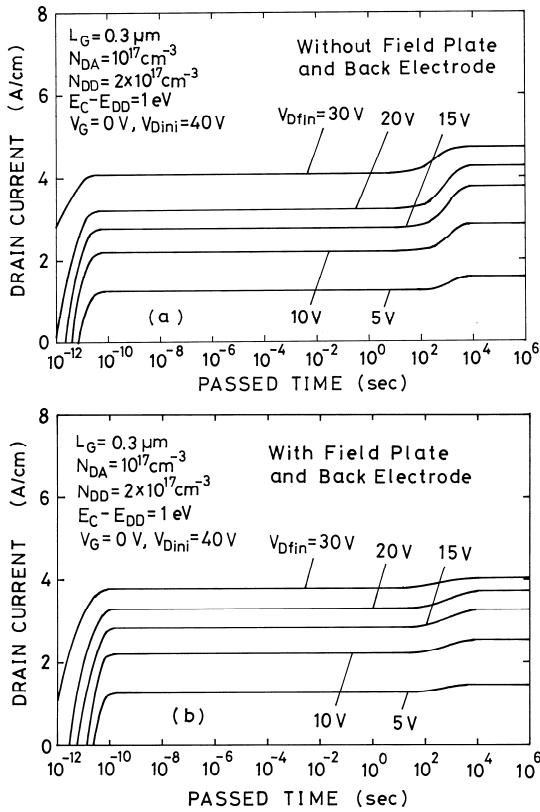


Figure 2: Calculated drain-current response characteristics of AlGaIn/GaN HEMTs when  $V_D$  is changed abruptly from 40 V to  $V_{Dfin}$  and  $V_G$  is kept constant at 0 V.  $N_{DA} = 10^{17} \text{ cm}^{-3}$ , (a) Without field plate and back electrode, (b) with field plate and back electrode ( $V_B = 0 \text{ V}$ ).

Fig.2(b) shows the case with a field plate and a back electrode. The drain currents remain low for some periods and gradually increase, showing drain-lag behavior. It is understood that the drain current begins to increase when the deep donors in the buffer layer begin to emit electrons. It is clearly seen that the drain-lag rate is smaller for the case with a field plate and a back electrode. We also simulate a case when the gate voltage is also changed from an off point to 0 V. In this case, the drain current remains further lower, indicating gate-lag and current collapse behavior.

Fig.3 shows the current reduction rate  $\Delta I_D/I_D$  due to drain lag, gate lag or current collapse for three device structures. This figure shows that the lags and current collapse are remarkably reduced by introducing a field plate (center), and the current collapse and drain lag are further reduced by introducing a back electrode (right).

Fig.4 shows a comparison of electron density profiles at  $V_D = 40 \text{ V}$  and  $V_G = 0 \text{ V}$  for the three device structures. Fig.4(a) shows the case of normal structure without a field plate and a back electrode. Fig.4(b) shows the case of field-plate structure, and Fig.4(c) shows the case of the structure

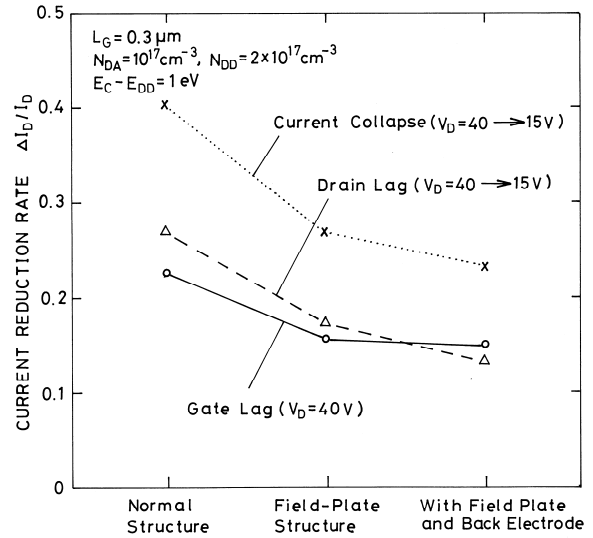


Figure 3: Current reduction rate  $\Delta I_D/I_D$  due to current collapse, drain lag or gate lag for three device structures.  $N_{DA} = 10^{17} \text{ cm}^{-3}$ .  $V_B = 0 \text{ V}$ .

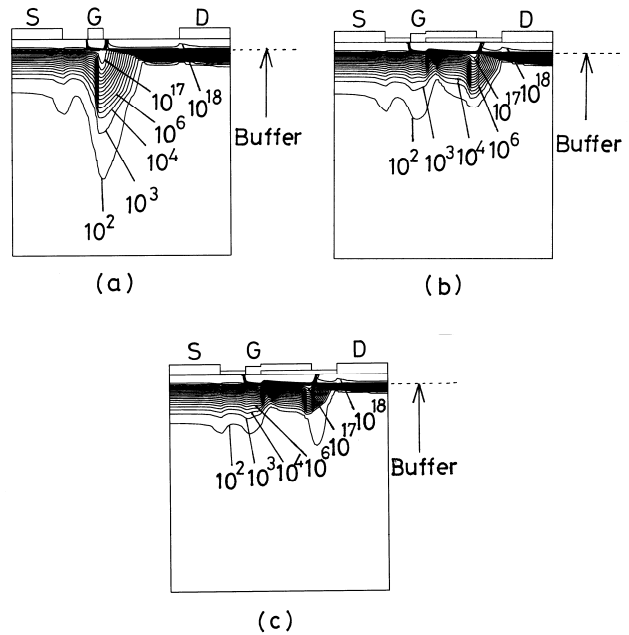


Figure 4: Electron density profiles at  $V_D = 40 \text{ V}$  and  $V_G = 0 \text{ V}$  for AlGaIn/GaN HEMTs with different device structures.  $N_{DA} = 10^{17} \text{ cm}^{-3}$  (a) Without field plate and back electrode, (b) with field plate and without backside electrode, (c) with field plate and backside electrode ( $V_B = 0 \text{ V}$ ).

with a field plate and a back electrode. In the normal structure (Fig.4(a)), electrons are injected rather deep into the buffer layer under the gate region. On the other hand, in the field-plate structure (Fig.4(b)), electrons are injected into the buffer layer under the drain edge of the field plate

as well as under the gate. But, the overall injection depth is not so deep as compared to the case without a field plate (Fig.4(a)). This is because the electric field at the drain edge of the gate is weakened. Hence, the trapping effects are reduced, leading to the smaller drain lag and current collapse. By further introducing a back electrode (Fig.4(c)), the electron injection under the gate is further reduced, leading to the additional reduction in drain lag and current collapse. This may be because the fixed potential at the backside electrode keeps the barrier from the channel toward the buffer high.

#### 4 CASES WITH RELATIVELY LOW ACCEPTOR DENSITIES

Figs.5(a) and 5(b) show the current reduction rate  $\Delta I_D/I_D$  due to drain lag, gate lag, or current collapse for the three device structures with  $N_{DA} = 2 \times 10^{16} \text{ cm}^{-3}$  and  $5 \times 10^{15} \text{ cm}^{-3}$ , respectively. When comparing with Fig.3, the reduction in lags and current collapse by introducing a field plate is not so significant. This is because electrons are diffused deeper into the buffer layer for lower  $N_{DA}$ , and hence the field plate can't control them well. On the other hand, the reduction in drain lag and current collapse by introducing a back electrode is more noticeable.

Fig.6 shows the conduction-band-edge energy profiles at  $V_D = 40 \text{ V}$  and  $V_G = 0 \text{ V}$  without and with the back electrode. Here,  $N_{DA} = 2 \times 10^{16} \text{ cm}^{-3}$ . Because of the fixed potential at the back electrode, the energy barrier for electrons from the channel toward the buffer is maintained at a high level when the drain voltage is applied. On the other hand, without the back electrode, the barrier at the channel-buffer interface can be lowered because the backside is floating. Therefore, we can say that with the use of back electrode, the barrier at the channel-buffer interface increases, and hence the electron injection into the buffer layer is weakened, thereby leading to reduced trapping effects and current collapse.

In conclusion, the introduction of field plate has been shown effective in reducing buffer-related current collapse when the acceptor density in the buffer layer is high. On the other hand, introducing a back electrode has been shown effective in reducing buffer-related current collapse when the acceptor density in the buffer layer is relatively low.

#### 5 DEPENDENCE OF BACK ELECTRODE VOLTAGE

Finally, we calculate the dependence of current collapse on the back electrode voltage  $V_B$ . Figure 7 shows the current reduction rate  $\Delta I_D/I_D$  due to current collapse for AlGaIn/GaN HEMTs as a function of the back electrode voltage  $V_B$ . Three cases with different  $N_{DA}$  are shown. The data without a back electrode are also shown for reference. It is seen that the decrease in current collapse when  $V_B$  becomes negative is not so significant for all the three cases. This is in contrast to the large reduction in current collapse

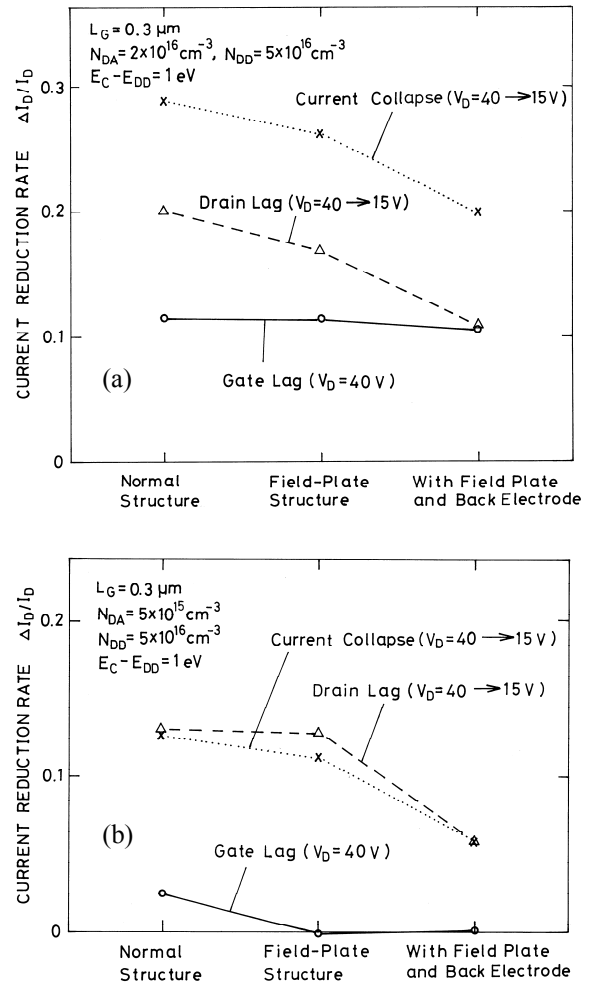


Figure 5: Current reduction rate  $\Delta I_D/I_D$  due to current collapse, drain lag, or gate lag for three device structures, where (a)  $N_{DA} = 2 \times 10^{16} \text{ cm}^{-3}$  and (b)  $N_{DA} = 5 \times 10^{15} \text{ cm}^{-3}$ .  $V_B = 0 \text{ V}$ .

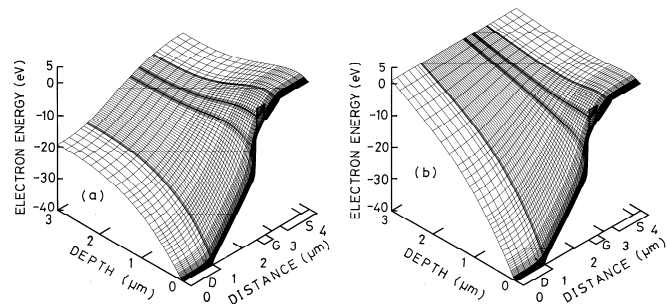


Figure 6: Conduction-band-edge energy profiles at  $V_D = 40 \text{ V}$  and  $V_G = 0 \text{ V}$  (a) without and (b) with back electrode ( $V_B = 0 \text{ V}$ ).  $N_{DA} = 2 \times 10^{16} \text{ cm}^{-3}$ .

when introducing the back electrode ( $V_B = 0 \text{ V}$ ).

Fig.8 shows a comparison of potential profiles of an AlGaIn/GaN HEMT with a back electrode between (a)  $V_B =$

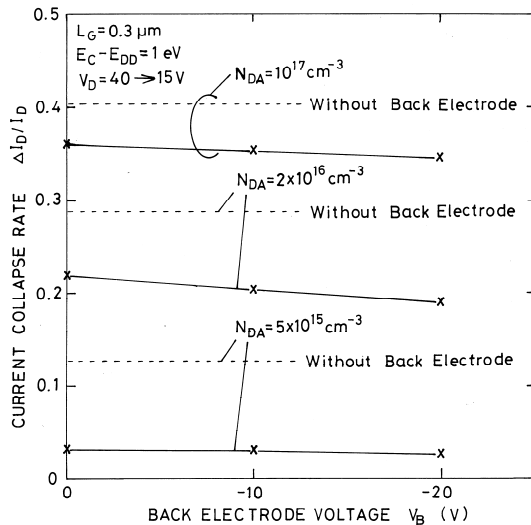


Figure 7: Current reduction rate  $\Delta I_D/I_D$  due to current collapse for field-plate AlGaIn/GaN HEMTs with different  $N_{DA}$  as a function of the back electrode voltage  $V_B$ .

0 V and (b)  $V_B = -20$  V. Here,  $V_D = 40$  V,  $V_G = 0$  V, and  $N_{DA} = 10^{17}$   $\text{cm}^{-3}$ . From Fig.8(b), we see that the back electrode voltage is entirely applied along the bulk of the buffer layer. This means that  $V_B$  does not almost affect the potential profiles at the channel-buffer interface and the current flow in the channel. Therefore,  $V_B$  does not almost affect the rate of current collapse in this case. This situation that the voltage is entirely applied along the bulk of buffer layer occurs because the deep donors act as electron traps. The same situation was observed when we calculated an GaAs n-i-n structure with a heavily compensated i-layer including deep donors “EL2” [9].

## 6 CONCLUSION

In this study, we performed two-dimensional transient analysis of field-plate AlGaIn/GaN HEMTs with a back electrode. It was shown that the field plate effectively reduced the current collapse when the acceptor density in the buffer layer was high. Moreover, the use of back electrode effectively reduced the current collapse particularly when the acceptor density in the buffer layer was relatively low because the fixed potential at the back electrode reduces electron injection into the buffer layer and the resulting trapping effects. However, increasing the negative back-electrode voltage was not so effective in reducing the current collapse because the voltage was entirely applied along the bulk of the buffer layer when the deep donors act as electron traps.

## REFERENCES

[1] S. C. Binari, P. B. Klein, and T. E. Kazior, “Trapping effects in GaN and SiC microwave FETs”, Proc. IEEE, vol.90, pp.1048-1058, 2002.

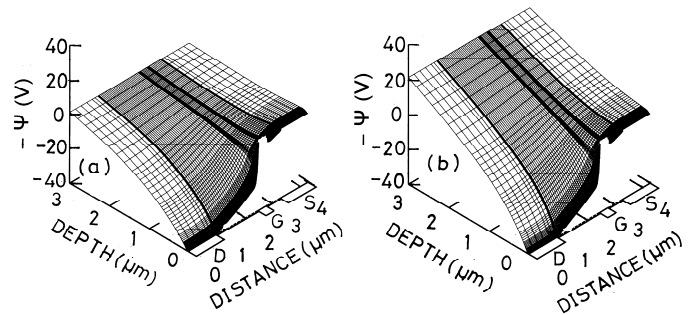


Figure 8: Comparison of potential profiles of field-plate AlGaIn/GaN HEMTs with a back electrode between (a)  $V_B = 0$  V and (b)  $V_B = -20$  V.  $V_D = 40$  V and  $V_G = 0$  V.  $N_{DA} = 10^{17}$   $\text{cm}^{-3}$ .

[2] U. K. Mishra, L. Shen, T. E. Kazior, and Y.-F. Wu, “GaN-based RF power devices and amplifiers”, Proc. IEEE, vol.96, pp.287-305, 2008.

[3] A. Koudymov, V. Adivarahan, J. Yang, G. Simon and M. A. Khan, “Mechanism of current collapse removal in field-plated nitride HFETs”, IEEE Electron Device Lett. vol.26, pp.704-706, 2005.

[4] K. Horio, A. Nakajima, and K. Itagaki, “Analysis of field-plate effects on buffer-related lag phenomena and current collapse in GaN MESFETs and AlGaIn/GaN HEMTs”, Semicond. Sci. Technol., vol.24, pp.085022-1–085022-7, 2009.

[5] W. Saito, T. Noda, M. Kuraguchi, Y. Takada, K. Tsuda, Y. Saito, I. Omura, M. Yamaguchi, “Effect of buffer layer structure on drain leakage current and current collapse phenomena in high-voltage GaN-HEMTs”, IEEE Trans. Electron Devices, vol.56, pp.1371-1376, 2009.

[6] K. Horio, H. Onodera, and A. Nakajima, “Analysis of backside-electrode and gate-field-plate effects on buffer-related current collapse in AlGaIn/GaN high electron mobility transistors”, J. Appl. Phys., vol.109, no.11, pp.114508-1–114508-7, 2011.

[7] K. Horio, K. Yonemoto, H. Takayanagi, and H. Nakano, “Physics-based simulation of buffer-trapping effects on slow current transients and current collapse in GaN field effect transistors” J. Appl. Phys., vol.98, no.12, pp.124502-1–124502-7, 2005.

[8] K. Horio and A. Nakajima, “Physical mechanism of buffer-related current transients and current slump in AlGaIn/GaN high electron mobility transistors”, Jpn. J. Appl. Phys., vol.47, pp.3428-3433, 2008.

[9] K. Horio, T. Ikoma and H. Yanai, “Computer-aided analysis of GaAs n-i-n structures with a heavily compensated i-layer”, IEEE Trans. Electron Devices, vol.ED-33, no.9, pp.1242-1250, 1986.